AU J.T. 12(4): 227-234 (Apr. 2009)

Dynamic Behavior of Compliant Slider Mechanism using the Pseudo-Rigid-Body Modeling Technique

Celestine Ikechukwu Ugwuoke, Sunday Matthew Abolarin and Vincent Obiajulu Ogwuagwu

Department of Mechanical Engineering,
Federal University of Technology, Minna, Niger State, Nigeria
E-mail: <ugwuokeikechukwu@yahoo.com; abolarinmatthew@yahoo.com; ovogwuagwu@yahoo.com>

Abstract

This work explores the use of the pseudo-rigid-body model to predict the dynamic behavior of compliant mechanisms. Based on the principle of dynamic equivalence, a simplified dynamic model for the compliant slider mechanism was developed using the pseudo-rigid-body modeling technique. Simulation results shows a very interesting discovery that there exist a range of frequencies over which the compliant slider mechanism exhibits better constant-force behavior than it does statically. For instance, at a frequency of 51 rad/s the compliant slider mechanism yields a median force of 307.62N with a force variance of ±3.9N, which is much better than the ±19.2N the device demonstrates statically.

Keywords: *Dynamic behavior, dynamic equivalence, compliant mechanisms, simulation, pseudo-rigid-body model.*

Introduction

Compliant mechanisms are mechanical devices which provide smooth and controlled motion guidance due to the deformation of some or all of the mechanism's components, they rely upon elastic deformation to perform their function of transmitting and/or transforming motion and force (Her and Midha 1987). Such mechanisms, with built-in flexible segments, are simpler and replace multiple rigid parts, pin joints, and add-on springs. Compliant mechanisms are relatively new class of mechanism (Kota *et al*. 1999). They may be multi-piece devices or monolithic (single-piece) devices and do not require sliding, rolling or other types of contact bearings often found in rigid mechanisms.

The pseudo-rigid-body model provides an easy way to model the complex nonlinear deflections of many compliant mechanisms (Howell 2001). The model approximates the force-deflection characteristics of a compliant segment using two or more rigid segments joined by pin joints, with torsional springs at the joints modeling the segment's stiffness (Jensen and Howell 2003). The usefulness of the pseudo-rigid-body model in allowing accurate analysis and synthesis of mechanism motion and energy storage characteristics has been abundantly demonstrated (Opdahl *et al*. 1998; Derderian *et al*. 996; Howell and Midha 1996; Lyon *et al*. 1997; Jensen *et al*. 1997; Mattlach and Midha 1996). While the model is very useful for the analysis of compliant mechanisms, its true power lies in the capability it gives for designing original compliant mechanisms (Jensen *et al*. 1997). This work explores the use of the pseudo-rigid-body model to predict the dynamic behavior of compliant slider mechanisms.

Dynamic Model Development

Mechanism Description

Figure 1(a) shows the compliant slider mechanism which consists of rigid links joined by small-length flexural pivots. Dividing the mechanism along the line of symmetry shows

that it consists of a pair of compliant slider mechanisms mounted to the same ground and sharing the same slider. Having two mechanisms opposite each other is useful because each cancels the moment induced by the other and the issue of friction between slider and ground is eliminated.

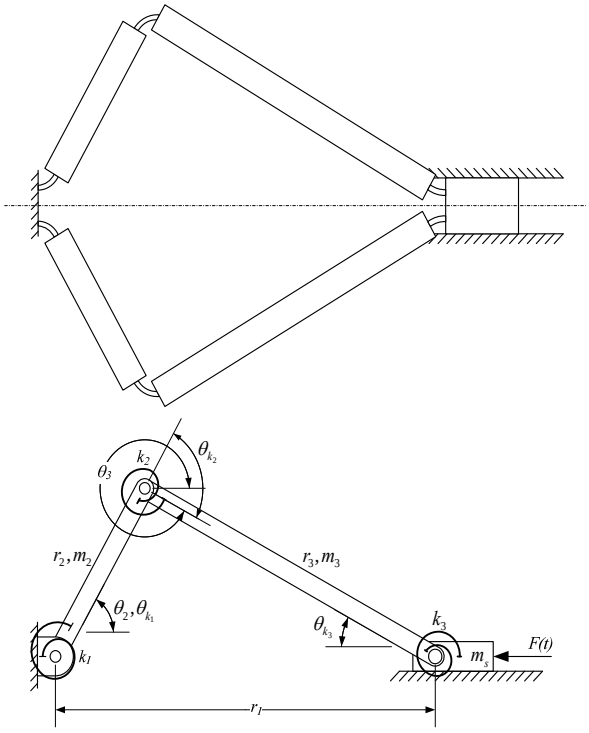

Fig. 1. (a) The compliant slider mechanism; and (b) its pseudo-rigid-body model.

Pseudo-Rigid-Body Model of Mechanism

The pseudo-rigid-body model of the compliant slider mechanism is shown in Fig. 1(b); only half of the symmetric mechanism is shown. The mechanism is converted to its rigid-body counterpart by using the pseudo-rigid-body model rule for small-length flexural pivots. The most straight forward alteration is that every small-length flexural pivot becomes a pin and torsional spring combination, centered at the middle of the flexible segment. The torsional spring constant K for small-length flexural pivots is given by

$$K = \frac{EI}{L}, \qquad (1)$$

where:
I is the moment of inertia of the cross section of the flexible segment;
E is the modulus of elasticity of the flexible segment;
L is the length of the flexible segment.

As seen in Fig. 1, application of the pseudo-rigid-body model rule to the mechanism does not result in a significant redistribution of its mass. Accordingly, dynamic inertial forces on the mechanism are reasonably consistent between the compliant mechanism and its pseudo-rigid-body model. It is assumed that no plastic deformation occurs as the mechanism cycles and the flexible segment deflects.

Position Analysis of Model

Figure 2 shows the position vector loop of model. Using complex number analysis, the vector loop equation is given as

$$R_2 + R_3 - R_1 = 0. \qquad (2)$$

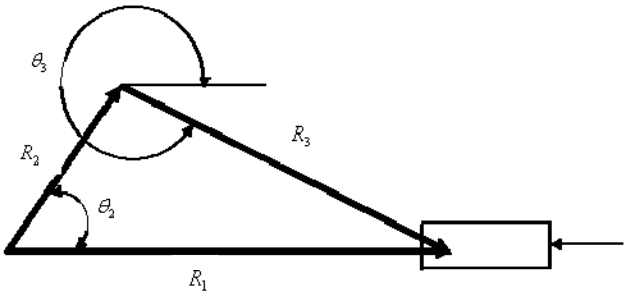

Fig. 2. Position vector loop of model.

Substituting the complex number equivalent for the position vectors, the following equation is obtained:

$$r_2 e^{j\theta_2} + r_3 e^{j\theta_3} - r_1 e^{j\theta_1} = 0. \qquad (3)$$

Substituting Euler equivalents, Eq. (3) becomes:

$$r_2(\cos\theta_2 + j\sin\theta_2) + r_3(\cos\theta_3 + j\sin\theta_3) - r_1(\cos\theta_1 + j\sin\theta_1) = 0. \qquad (4)$$

Separating real and imaginary components and further simplifying, the following relations are obtained:

$$r_1 = r_2\cos\theta_2 + r_3\cos\theta_3, \qquad (5)$$

$$\sin\theta_3 = -\frac{r_2}{r_3}\sin\theta_2, \qquad (6)$$

$$\cos\theta_3 = \frac{1}{r_3}\sqrt{r_3^2 - r_2^2\sin^2\theta_2}. \qquad (7)$$

Velocity Analysis of Model

Differentiating Eq. (3) with respect to time and noting that r_2, r_3 and θ_1 are constants, and r_1 varies with time, the following equation is obtained:

$$jr_2e^{j\theta_2}\dot{\theta}_2+jr_3e^{j\theta_3}\dot{\theta}_3-\dot{r}_1=0, \quad (8)$$

where: $\dot{r}_1$ = linear velocity of the slider.
Substituting Euler equivalent, Eq. (8) becomes:

$$jr_2(\cos\theta_2+j\sin\theta_2)\dot{\theta}_2 + jr_3(\cos\theta_3+j\sin\theta_3)\dot{\theta}_3-\dot{r}_1=0. \quad (9)$$

Simplifying Eq. (9), gives

$$r_2(-\sin\theta_2+j\cos\theta_2)\dot{\theta}_2 + r_3(-\sin\theta_3+j\cos\theta_3)\dot{\theta}_3-\dot{r}_1=0. \quad (10)$$

Separating real and imaginary components and simplifying gives the following relations:

$$\dot{\theta}_3=-\frac{r_2\dot{\theta}_2\cos\theta_2}{\sqrt{r_3^2-r_2^2\sin^2\theta_2}}, \quad (11)$$

$$\dot{r}_1=-r_2\dot{\theta}_2\sin\theta_2-\frac{r_2^2\dot{\theta}_2\sin\theta_2\cos\theta_2}{\sqrt{r_3^2-r_2^2\sin^2\theta_2}}. \quad (12)$$

Equation (8) is the velocity difference equation which is given as:

$$V_2+V_{32}-V_{SLIDER}=0, \quad (13)$$

$$V_{SLIDER}=V_2+V_{32}. \quad (14)$$

The absolute velocity of link 2 and the velocity difference of link 3 with respect to link 2 is obtained from Eq. (13), and given as:

$$V_2=jr_2e^{j\theta_2}\dot{\theta}_2, \quad (15)$$

$$V_{32}=jr_3e^{j\theta_3}\dot{\theta}_3, \quad (16)$$

$$V_{SLIDER}=jr_2e^{j\theta_2}\dot{\theta}_2+jr_3e^{j\theta_3}\dot{\theta}_3. \quad (17)$$

The absolute velocity of the centre of mass of link 2 is therefore:

$$V_{C2}=j\frac{r_2}{2}e^{j\theta_2}\dot{\theta}_2. \quad (18)$$

Substituting Euler equivalent and simplifying, Eq. (18) becomes:

$$V_{C2}=\frac{1}{2}r_2\dot{\theta}_2. \quad (19)$$

The absolute velocity of the centre of mass of link 3 is therefore:

$$V_{C3}=jr_2e^{j\theta_2}\dot{\theta}_2+j\frac{r_3}{2}e^{j\theta_3}\dot{\theta}_3. \quad (20)$$

Substituting Euler equivalent and simplifying, Eq. (20) becomes:

$$V_{C3}=\left(r_2^2\dot{\theta}_2^2+r_2r_3\cos(\theta_2-\theta_3)\dot{\theta}_2\dot{\theta}_3+\frac{1}{4}r_3^2\dot{\theta}_3^2\right)^{\frac{1}{2}}. \quad (21)$$

Acceleration Analysis of Model

Differentiating Eq. (8) gives an expression for the acceleration:

$$\left(jr_2\ddot{\theta}_2e^{j\theta_2}+j^2r_2\dot{\theta}_2^2e^{j\theta_2}\right) + \left(jr_3\ddot{\theta}_3e^{j\theta_3}+j^2r_3\dot{\theta}_3^2e^{j\theta_3}\right)-\ddot{r}_1=0. \quad (22)$$

Simplifying, Eq. (22) becomes:

$$\left(jr_2\ddot{\theta}_2e^{j\theta_2}-r_2\dot{\theta}_2^2e^{j\theta_2}\right) + \left(jr_3\ddot{\theta}_3e^{j\theta_3}-r_3\dot{\theta}_3^2e^{j\theta_3}\right)-\ddot{r}_1=0. \quad (23)$$

Substituting Euler equivalent, the following expression is obtained:

$$r_2\ddot{\theta}_2(-\sin\theta_2+j\cos\theta_2) - r_2\dot{\theta}_2^2(\cos\theta_2+j\sin\theta_2) + r_3\ddot{\theta}_3(-\sin\theta_3+j\cos\theta_3) - r_3\dot{\theta}_3^2(\cos\theta_3+j\sin\theta_3)-\ddot{r}_1=0. \quad (24)$$

Separating real and imaginary components and simplifying:

$$\ddot{r}_1=-r_2\ddot{\theta}_2\sin\theta_2-r_2\dot{\theta}_2^2\cos\theta_2 - r_3\ddot{\theta}_3\sin\theta_3-r_3\dot{\theta}_3^2\cos\theta_3, \quad (25)$$

$$\ddot{\theta}_3=\frac{-r_2\ddot{\theta}_2\cos\theta_2+r_2\dot{\theta}_2^2\sin\theta_2+r_3\dot{\theta}_3^2\sin\theta_3}{r_3\cos\theta_3}. \quad (26)$$

Equation (23) is the acceleration difference equation which is given as:

$$A_2+A_{32}-A_{SLIDER}=0. \quad (27)$$

The absolute acceleration of link 2 and the acceleration difference of link 3 with respect to link 2 is obtained from Eq. (27), and given as:

$$A_2 = \left(A_2^t + A_2^n\right) = \left(jr_2 \ddot{\theta}_2 e^{j\theta_2} - r_2 \dot{\theta}_2^2 e^{j\theta_2} \right), \quad (28)$$

$$A_{32} = \left(A_{32}^t + A_{32}^n\right) = \left(jr_3 \ddot{\theta}_3 e^{j\theta_3} - r_3 \dot{\theta}_3^2 e^{j\theta_3} \right), \quad (29)$$

$$A_{SLIDER} = \ddot{r}_1 = A_2 + A_{32}. \quad (30)$$

The absolute acceleration of the centre of mass of link 2 is therefore:

$$A_{C2} = \left(j\frac{r_2}{2}\ddot{\theta}_2 e^{j\theta_2} - \frac{r_2}{2}\dot{\theta}_2^2 e^{j\theta_2} \right). \quad (31)$$

Substituting Euler equivalent and simplifying, Eq. (31) becomes:

$$A_{C2} = \frac{1}{2} r_2 \left(\ddot{\theta}_2^2 + \dot{\theta}_2^4 \right)^{\frac{1}{2}}. \quad (32)$$

The absolute acceleration of the centre of mass of link 3 is therefore:

$$A_{C3} = \left(jr_2 \ddot{\theta}_2 e^{j\theta_2} - r_2 \dot{\theta}_2^2 e^{j\theta_2} \right) + \left(j\frac{r_3}{2}\ddot{\theta}_3 e^{j\theta_3} - \frac{r_3}{2}\dot{\theta}_3^2 e^{j\theta_3} \right). \quad (33)$$

Substituting Euler equivalent and simplifying, Eq. (33) becomes

$$A_{C3} = \left[r_2^2 \left(\ddot{\theta}_2^2 + \dot{\theta}_2^4 \right) + r_2 r_3 \cos(\theta_2 - \theta_3) \ddot{\theta}_2 \ddot{\theta}_3 + r_2 r_3 \sin(\theta_2 - \theta_3) \ddot{\theta}_2 \dot{\theta}_3^2 - r_2 r_3 \sin(\theta_2 - \theta_3) \dot{\theta}_2^2 \ddot{\theta}_3 + r_2 r_3 \cos(\theta_2 - \theta_3) \dot{\theta}_2^2 \dot{\theta}_3^2 + \frac{1}{4} r_3^2 \left(\ddot{\theta}_3^2 + \dot{\theta}_3^4 \right) \right]^{\frac{1}{2}}. \quad (34)$$

Potential Energy Formulation for Model

Using the pseudo-rigid-body model, the potential energy equation can easily be found (Jensen and Howell 2003). For a segment modeled using a torsional spring and a pin joint, the potential energy V stored in the segment is given by:

$$V = \frac{1}{2} K \theta_K^2, \quad (35)$$

where K is the torsional spring constant and θ_K is the pseudo-rigid-body angle or the angle of deflection of the compliant segment.

The total potential energy in the mechanism is therefore the sum of the potential energy stored in each compliant segment:

$$V = \sum_{i=2}^{n} V_i = \frac{1}{2} \sum_{i=2}^{n} \left(K_i \theta_{Ki}^2 \right), \quad (36)$$

where i = 2, 3,…, n enumerates all torsional springs.

For the model, the potential energy equation is given as:

$$V = \frac{1}{2} \left(K_1 \theta_{K1}^2 + K_2 \theta_{K2}^2 + K_3 \theta_{K3}^2 \right), \quad (37)$$

where K_1, K_2 and K_3 are the torsional spring constants and θ_{K1}, θ_{K2} and θ_{K3} are the relative deflections of the torsional springs given as:

$$\theta_{K1} = \theta_2, \quad (38)$$

$$\theta_{K2} = \theta_2 + \sin^{-1}\left(\frac{r_2}{r_3} \sin\theta_2 \right), \quad (39)$$

$$\theta_{K3} = \sin^{-1}\left(\frac{r_2}{r_3} \sin\theta_2 \right). \quad (40)$$

Kinetic Energy Formulation for Model

As shown in Fig. 3, the centre of mass of each link is moving with linear velocity and the link is also rotating about the centre of mass with angular velocity. The total kinetic energy for any given link is therefore, the sum of the translational and rotational kinetic energies:

$$T_{\text{total for each link}} = T_{\text{translation}} + T_{\text{rotation}} = \frac{1}{2} m V_C^{\,2} + I_C \dot{\theta}^2. \quad (41)$$

For any mechanism, the total kinetic energy is given by:

$$T = \sum_{i=2}^{n} T_i = \frac{1}{2} \sum_{i=2}^{n} \left(m_i V_{Ci}^2 + I_{Ci} \dot{\theta}_i^2 \right), \quad (42)$$

where i = 2, 3,…, n enumerates all moving links.

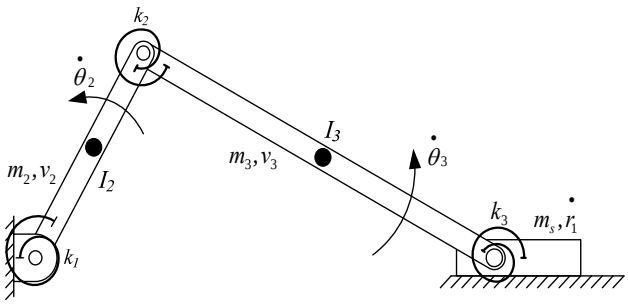

Fig. 3. Translational and rotational motion of the mechanism link.

For the model, the kinetic energy equation is given as:

$$T = \frac{1}{2}m_2 V_{C2}^2 + \frac{1}{2}m_3 V_{C3}^2 + \frac{1}{2}m_s \dot{r}_1^2 + \frac{1}{2}I_{C2}\dot{\theta}_2^2 + \frac{1}{2}I_{C3}\dot{\theta}_3^2 , \quad (43)$$

where:

m_i = mass of links 2 and 3;

V_{Ci} = velocity of the center of mass of links 2 and 3;

I_{Ci} = mass moment of inertia of links 2 and 3 about the center of mass;

$\dot{\theta}_i$ = angular velocity of links 2 and 3;

$\dot{r}_1$ = velocity of the slider.

The first three terms of the kinetic energy expression represent the translational energy of the system, and the last two represent the rotational energy. The mass moments of inertia of links 2 and 3 about the center of mass is given by:

$$I_{Ci} = \frac{1}{12}m_i r_i^2 . \quad (44)$$

Lagrange's Equation Formulation

Lagrange's method is one of the most useful techniques in generating equations of motion of mechanisms, especially when internal forces and reactions are not of interest (Sandor and Erdman, 1988). The compact form of Lagrange's equation is given as

$$\frac{d}{dt}\left(\frac{\partial \ell}{\partial \dot{q}_r}\right) - \frac{\partial \ell}{\partial q_r} + \frac{\partial K}{\partial \dot{q}_r} = F_{q_r} , \quad (45)$$

where: q_r = Generalized position coordinates.

There are as many Lagrange's equations of motion as there are degrees of freedom in the system. The uniform standard form of these equations holds no matter how complicated the relation between the kinematics constraints and the generalized coordinates. Infact, one can strategically choose a set of coordinates to facilitate algebraic manipulation due to the invariance of the form of the equations with respect to the choice of generalized coordinates. Taking θ_2 as the generalized position coordinate and neglecting the effect of damping on mechanism, Lagrange's equation becomes

$$\frac{d}{dt}\left(\frac{\partial \ell}{\partial \dot{\theta}_2}\right) - \frac{\partial \ell}{\partial \theta_2} = M_{\theta_2} . \quad (46)$$

Assuming a conservative system, the Lagrangian ℓ given below is formed by taking the difference of the scalar quantities of kinetic energy T and potential energy V of the system:

$$\ell = T - V . \quad (47)$$

Because θ_2 is the only independent coordinate in a single-degree-of-freedom mechanism, the velocity of the centre of mass and the angular velocity for the i^{th} link is a function only of θ_2 and $\dot{\theta}_2$ (Sandor and Erdman, 1988). The following equations recast the variables in T and V in terms of θ_2 and $\dot{\theta}_2$:

$$V_{C2}^2 = \frac{1}{4}r_2^2 \dot{\theta}_2^2 , \quad (48)$$

$$V_{C3}^2 = r_2^2 \sin^2\theta_2 \dot{\theta}_2^2 + \frac{1}{4}\frac{r_2^2 r_3^2 \cos^2\theta_2}{r_3^2 - r_2^2 \sin^2\theta_2}\dot{\theta}_2^2 + \frac{r_2^3 \sin^2\theta_2 \cos\theta_2}{\sqrt{r_3^2 - r_2^2 \sin^2\theta_2}}\dot{\theta}_2^2 , \quad (49)$$

$$r_1 = r_2 \cos\theta_2 + \sqrt{r_3^2 - r_2^2 \sin^2\theta_2} , \quad (50)$$

$$\dot{r}_1 = -r_2 \sin\theta_2 \dot{\theta}_2 - \frac{r_2^2 \sin\theta_2 \cos\theta_2}{\sqrt{r_3^2 - r_2^2 \sin^2\theta_2}}\dot{\theta}_2 , \quad (51)$$

$$\dot{r}_1^2 = r_2^2 \sin^2\theta_2 \dot{\theta}_2^2 + \frac{r_2^4 \sin^2\theta_2 \cos^2\theta_2}{r_3^2 - r_2^2 \sin^2\theta_2}\dot{\theta}_2^2 + \frac{2r_2^3 \sin^2\theta_2 \cos\theta_2}{\sqrt{r_3^2 - r_2^2 \sin^2\theta_2}}\dot{\theta}_2^2 , \quad (52)$$

$$\theta_3 = \sin^{-1}\left(-\frac{r_2}{r_3}\sin\theta_2\right), \quad (53)$$

$$\dot{\theta}_3 = -\frac{r_2\cos\theta_2}{\sqrt{r_3^2 - r_2^2\sin^2\theta_2}}\dot{\theta}_2, \quad (54)$$

$$\dot{\theta}_3^2 = \frac{r_2^2\cos^2\theta_2}{r_3^2 - r_2^2\sin^2\theta_2}\dot{\theta}_2^2. \quad (55)$$

The Lagrangian ℓ for the model is therefore

$$\ell = \frac{1}{2}m_2V_{C2}^2 + \frac{1}{2}m_3V_{C3}^2 + \frac{1}{2}m_s\dot{r}_1^2 + \frac{1}{2}I_{C2}\dot{\theta}_2^2 + \frac{1}{2}I_{C3}\dot{\theta}_3^2 - \frac{1}{2}K_1\theta_{K1}^2 - \frac{1}{2}K_2\theta_{K2}^2 - \frac{1}{2}K_3\theta_{K3}^2. \quad (56)$$

Lagrange's formulation requires that the partial derivatives of the Lagrangian ℓ with respect to the generalized coordinate θ_2 and its time derivative $\dot{\theta}_2$ be carried out to form the equation of motion for the system. When the derivatives of the Lagrangian are expanded out and simplified, the dynamic equation of motion for the system is obtained which is given as:

$$\left[m_2\left(\frac{1}{4}r_2^2\right) + m_3\left(\frac{r_2^3\sin^2\theta_2\cos\theta_2}{\sqrt{r_3^2 - r_2^2\sin^2\theta_2}} + \frac{1}{4}\frac{r_2^2r_3^2\cos^2\theta_2}{r_3^2 - r_2^2\sin^2\theta_2} + r_2^2\sin^2\theta_2\right)\right.$$
$$+ m_S\left(\frac{r_2^4\sin^2\theta_2\cos^2\theta_2}{r_3^2 - r_2^2\sin^2\theta_2} + 2\frac{r_2^3\sin^2\theta_2\cos\theta_2}{\sqrt{r_3^2 - r_2^2\sin^2\theta_2}} + r_2^2\sin^2\theta_2\right) + I_{C2} + I_{C3}\frac{r_2^2\cos^2\theta_2}{r_3^2 - r_2^2\sin^2\theta_2}\Bigg]\ddot{\theta}_2$$
$$+\left[m_3\left(\frac{1}{2}\frac{r_2^5\sin^3\theta_2\cos^2\theta_2}{\left(r_3^2 - r_2^2\sin^2\theta_2\right)^{3/2}} + \frac{1}{4}\frac{r_2^4r_3^2\sin\theta_2\cos^3\theta_2}{\left(r_3^2 - r_2^2\sin^2\theta_2\right)^2} - \frac{1}{2}\frac{r_2^3\sin^3\theta_2}{\sqrt{r_3^2 - r_2^2\sin^2\theta_2}}\right.\right.$$
$$+\frac{r_2^3\sin\theta_2\cos^2\theta_2}{\sqrt{r_3^2 - r_2^2\sin^2\theta_2}} - \frac{1}{4}\frac{r_2^2r_3^2\sin\theta_2\cos\theta_2}{r_3^2 - r_2^2\sin^2\theta_2} + r_2^2\sin\theta_2\cos\theta_2\Bigg) + m_S\left(\frac{r_2^6\sin^3\theta_2\cos^3\theta_2}{\left(r_3^2 - r_2^2\sin^2\theta_2\right)^2}\right.$$
$$+\frac{r_2^5\sin^3\theta_2\cos^2\theta_2}{\left(r_3^2 - r_2^2\sin^2\theta_2\right)^{3/2}} - \frac{r_2^4\sin^3\theta_2\cos\theta_2}{r_3^2 - r_2^2\sin^2\theta_2} + \frac{r_2^4\sin\theta_2\cos^3\theta_2}{r_3^2 - r_2^2\sin^2\theta_2} + 2\frac{r_2^3\sin\theta_2\cos^2\theta_2}{\sqrt{r_3^2 - r_2^2\sin^2\theta_2}}$$
$$\left.\left.\left. - \frac{r_2^3\sin^3\theta_2}{\sqrt{r_3^2 - r_2^2\sin^2\theta_2}} + r_2^2\sin\theta_2\cos\theta_2\right) + I_{C3}\left(\frac{r_2^4\sin\theta_2\cos^3\theta_2}{\left(r_3^2 - r_2^2\sin^2\theta_2\right)^2} - \frac{r_2^2\sin\theta_2\cos\theta_2}{r_3^2 - r_2^2\sin^2\theta_2}\right)\right]\dot{\theta}_2^2$$
$$+K_1\theta_2 + K_2\left(\theta_2 + \sin^{-1}\left(\frac{r_2}{r_3}\sin\theta_2\right)\right)\left(1 + \frac{r_2\cos\theta_2}{\sqrt{r_3^2 - r_2^2\sin^2\theta_2}}\right) + \frac{K_3\sin^{-1}\left(\frac{r_2}{r_3}\sin\theta_2\right)r_2\cos\theta_2}{\sqrt{r_3^2 - r_2^2\sin^2\theta_2}} = M_{\theta 2}. \quad (57)$$

Torque $M_{\theta 2}$ is transformed to mechanism's output force F using the power relationship given as:

$$F\dot{r}_1 = M_{\theta 2}\dot{\theta}_2, \quad (58)$$

$$F = \frac{\tau_F}{\left(\frac{\partial r_1}{\partial\theta_2}\right)}, \quad (59)$$

where:

$$\frac{\partial r_1}{\partial\theta_2} = -r_2\sin\theta_2 - \frac{r_2^2\sin\theta_2\cos\theta_2}{\sqrt{r_3^2 - r_2^2\sin^2\theta_2}}. \quad (60)$$

Equations (57)–(60) represent the dynamic model of the compliant slider mechanism. Note that the equation of motion was derived from the pseudo-rigid-body model of the mechanism, rather than the actual compliant mechanism.

Results and Discussion

Table 1 shows the mechanism parameters used for the simulation. Position plot representing the sinusoidal input and position force diagram are shown in Figs. 4 and 5.

Table 1. Mechanism parameters.

Mechanism Parameters	Parameter Value
r_2	90 mm
r_3	120 mm
m_2	0.026kg
m_3	0.037 kg
m_s	0.087kg
b	30 mm
h	0.65 mm
I	6.866 x 10^{-13} m^4
E	207 Gpa

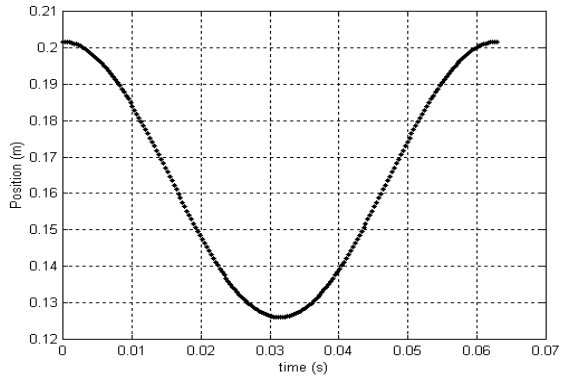

Fig. 4. Position plot representing the sinusoidal input.

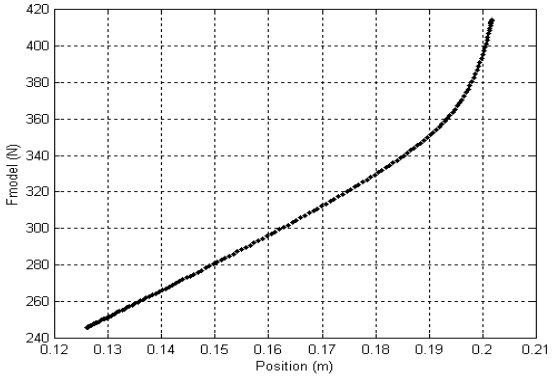

Fig. 5. Position force diagram.

In the evaluation of the dynamic model, three useful plots are analyzed, the mean force, the median force and the peak-to-peak force difference of the dynamic model as a function of frequency, this is shown in Figs. 6, 7 and 8. The frequency assumes a sinusoidal position input with amplitude equal to 40% mechanism deflection with a slight pre-displacement to give a pre-load at full expansion. Notice that the curve in the peak-to-peak force plot first curves down, before it starts to increase.

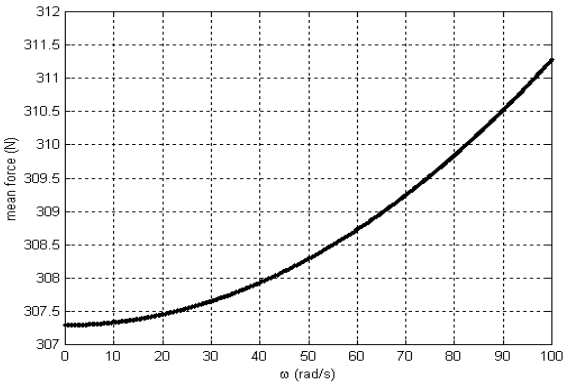

Fig. 6. The mean force as a function of frequency.

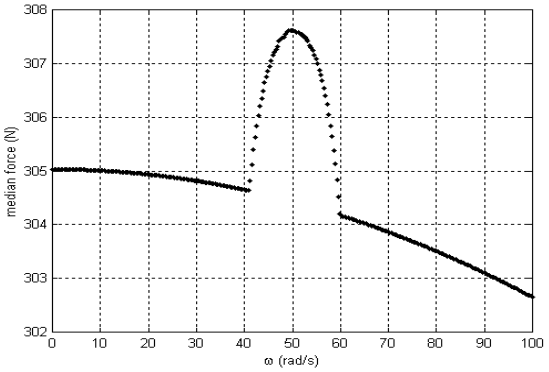

Fig. 7. The median force as a function of frequency.

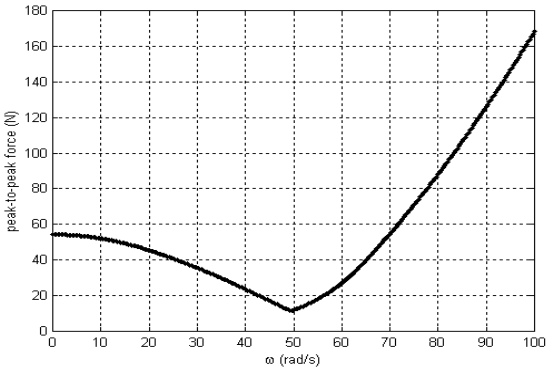

Fig. 8. The peak-to-peak force difference as a function of frequency.

This is a very interesting discovery of the peak-to-peak force plot which shows that there is a range of frequencies over which a compliant slider mechanism exhibits better constant-force behavior. This interesting discovery will significantly improve the likelihood that the compliant slider mechanism could be viable in industry for constant-force applications. For instance, at a frequency of 51

rad/s as demonstrated in Fig. 8, the compliant slider mechanism will yield a median force of 307.62N with a force variance of ±3.9N as demonstrated clearly in Fig. 9, which is much better than the ±19.2N the device demonstrates statically. This better constant-force behavior is likely due to inertial effects.

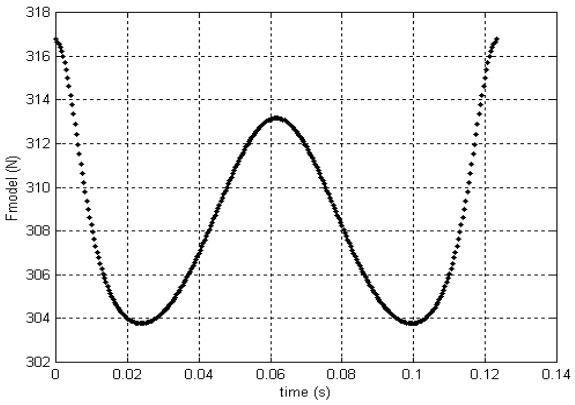

Fig. 9. Predicted force for sinusoidal input of ω = 51 *rad/*s.

Conclusion

Much work is actually needed for a further study on the dynamic analysis of compliant mechanisms to improve on their operational performance. Based on the principle of dynamic equivalence, a simplified dynamic model for the compliant slider mechanism was developed using the pseudo-rigid-body modeling technique. Simulation results shows a very interesting discovery that there exist a range of frequencies over which a compliant slider mechanism exhibits better constant-force behaviour than it does statically. This interesting discovery will significantly improve the likelihood that the compliant slider mechanism could be viable in industry for constant-force applications.

References

Derderian, J.M.; Howell, L.L.; Murphy, M.D.; Lyon, S.M.; and Pack, S.D. 1996. Compliant parallel-guiding mechanisms. Proc. 1996 ASME Design Engineering Technical Conf., 96-DETC/MECH-1208.

Her, I.; and Midha, A. 1987. A Compliance number concept for compliant mechanisms, and type synthesis. J. Mech. Transm. Autom. in Design, Trans ASME 109(3): 348-55.

Howell, L.L. 2001. Compliant Mechanisms. John Wiley & Sons, New York, NY, USA.

Howell, L.L.; and Midha, A. 1996. A Loop-Closure Theory for the Analysis and Synthesis of Compliant Mechanisms, ASME J. Mech. Design 118(1): 121-5.

Jensen, B.D.; and Howell, L.L. 2003, Identification of compliant pseudo-rigid-body four-link mechanism configurations resulting in bistable behavior. J. Mech. Design, Trans. ASME 125: 701.

Jensen, B.D.; Howell, L.L.; Gunyan, D.B.; and Salmon, L.G. 1997. The Design and Analysis of Compliant MEMS Using the Pseudo-Rigid-Body Model, Microelectro-mechanical Systems (MEMS) 1997, presented at the 1997 ASME International Mechanical Engineering Congress and Exposition, 16-21 November 1997, Dallas, TX, DSC-Vol. 62, pp. 119-126.

Lyon, S.M.; Evans, M.S.; Erickson, P.A.; and Howell, L.L. 1997. Dynamic Response of Compliant Mechanisms Using the Pseudo-Rigid-Body Model, Proceedings of the 1997 ASME Design Engineering Technical Conferences, DETC97/VIB-4177.

Mettlach, G.A.; and Midha, A. 1996, Using Burmester Theory in the Design of Compliant Mechanisms, Proceedings of the 1996 ASME Design Engineering Technical Conferences, 96-DETC/MECH-1181.

Opdahl, P.G.; Jensen, B.D.; and Howell, L.L. 1998. An investigation into compliant bistable mechanisms. Proc. 1998 ASME Design Engin. Tech. Conf. DETC98/ MECH-5914.

Sandor, G.N.; and Erdman, A.G. 1988. Advanced Mechanism Design: Analysis and Synthesis, Volume 2, Prentice-Hall, New Delhi, India, pp. 396-397, 466.

Kota, S., Hetrick, J.; Z. Li.; and Saggere, L. 1999. Tailoring unconventional actuators with compliant transmissions: Design methods and applications, ASME/IEEE J. Mechatronics 4: 396-408.